

RSRM Nozzle Actuator Bracket/ Lug Fracture Mechanics Qualification Test Final Report

July 1993

Prepared for

National Aeronautics and Space Administration
George C. Marshall Space Flight Center
Marshall Space Flight Center, Alabama 35812

Contract No. NAS8-30490
DR No. 5-3
WBS No. HQ301 05 07
ECS No. SS1253

Thiokol CORPORATION
SPACE OPERATIONS

P.O. Box 707, Brigham City, UT 84302-0707 (801) 863-3511

N94-17080

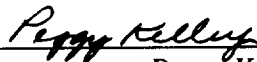
Unclass

G3/20 0193042

(NASA-CR-193859) RSRM NOZZLE
ACTUATOR BRACKET/LUG FRACTURE
MECHANICS QUALIFICATION TEST Final
Report (Thiokol Corp.) 53 p

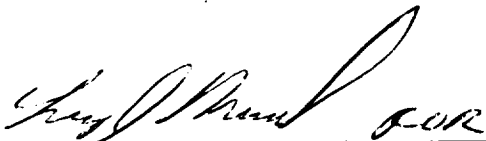
**RSRM Nozzle Actuator Bracket/
Lug Fracture Mechanics Qualification
Test Final Report**

Prepared by:



Peggy Kelley
Systems Planning and Interfaces

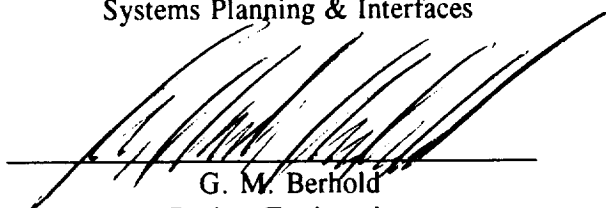
Approved by:



D. E. Campbell
Systems Planning & Interfaces



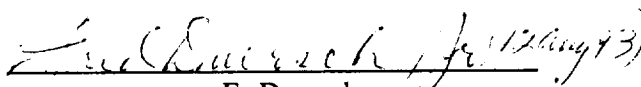
T. Nhan
Structural Analysis



G. M. Berhold
Project Engineering



T. K. Lai
RSRM Fracture Control
Technical Subcommittee



F. Duersch
Systems Assurance



G. E. Paul
Requirements and Verifications

 8/12/93

Data Management/Release
ECS No. SS1253

CONTENTS

<u>Section</u>	<u>Page</u>
1 INTRODUCTION	1
2 TEST OBJECTIVES	2
3 EXECUTIVE SUMMARY	3
3.1 SUMMARY	3
3.2 CONCLUSIONS	3
3.2.1 Phase 1 Conclusions	3
3.2.2 Phase 2 Conclusions	4
3.3 RECOMMENDATIONS	4
4 INSTRUMENTATION	7
5 PHOTOGRAPHY	7
6 TEST ITEM DESCRIPTION	8
6.1 PHASE 1 TESTING	8
6.2 PHASE 2 TESTING	8
7 RESULTS AND DISCUSSION	14
7.1 PHASE 1	14
7.1.1 Analytical Model	14
7.1.2 Critical Loads	14
7.2 PHASE 2	22
8 APPLICABLE DOCUMENTS	25

Attachments

A	Thiokol Memos L633-FY93-M112-Rev A and L711-FY93-M348	A-1
B	NASA Memo SA51(192-90): Actuator Bracket Gracture Mechanics Testing . .	B-1

FIGURES

<u>Figure</u>		<u>Page</u>
1	Phase 1 Testing Results	4
2	Specimen 2-1 Starter Notch Location	5
3	Specimen 2-2 Starter Notch Location	6
4	Square Lug Model/Test Specimen Geometry and Dimensions	9
5	Comparison of Analytical Model to Actuator Bracket	10
6	Phase 1 Test Specimen	11
7	Phase 1 Test Fixture	12
8	Phase 2 Test Specimen and Configuration	13
9	Comparison of Failure Load Versus Crack Area	17
10	Phase 1 Post-test, Specimen 1	19
11	Phase 1 Post-test, Specimen 2	20
12	Phase 1 Post-test, Specimen 3	21
13	Phase 1 Post-test, Specimen 4	22
14	Phase 1 Post-test, Specimen 5	23
15	Phase 1 Post-test, Specimen 6	24

TABLES

<u>Table</u>		<u>Page</u>
1	Flight Load Spectrum	23

1 / INTRODUCTION

This is the final report for the actuator bracket/lug fracture mechanics qualification test. The test plan (CTP-0071) outlined a two-phase test program designed to answer questions about the fracture criticality of the redesigned solid rocket motor (RSRM) nozzle actuator bracket. An analysis conducted using the NASA/FLAGRO fracture mechanics computer program indicated that the actuator bracket might be a fracture critical component.

In the NASA/FLAGRO analysis, a simple lug model was used to represent the actuator bracket. It was calculated that the bracket would fracture if subjected to an actuator stall load in the presence of a 0.10-in. corner crack at the actuator attachment hole. The 0.10-in. crack size corresponds to the nondestructive inspection detectability limit for the actuator bracket. The inspection method used is the dye penetrant method. The actuator stall load (103,424 lb) is the maximum load which the actuator bracket is required to withstand during motor operation.

This testing was designed to establish the accuracy of the analytical model and to directly determine whether the actuator bracket is capable of meeting fracture mechanics safe-life requirements.

2 / TEST OBJECTIVES

The RSRM nozzle actuator bracket/lug fracture mechanics test was a Type 1 qualification test.

The test objectives for each of the two distinct phases of the test are defined by test summary sheets SRX-13.0 and TRX-7.0 of the Development and Verification Plan for the RSRM (TWR-15723, Rev 8).

Phase 1

Specific development test objectives included:

- A. Verifying lug fracture predictions of NASA/FLAGRO linear elastic fracture mechanics analytical model.
- B. Determining critical load in square lug specimen for various initial crack sizes.
- C. Determining the acceptability of the lug model for analyzing the actuator bracket.

Phase 2

The specific qualification objective was to:

- D. Verify capability of actuator bracket to undergo four cycles of the flight load spectrum with a 0.10-in. preexisting crack (Reference TWR-16875).

Specific development test objectives were:

- E. Determining critical load for actuator bracket with a 0.1-in. crack.
- F. Determining the critical flaw size in the actuator bracket at actuator stall load (103,424 lb).

3 / EXECUTIVE SUMMARY

3.1 SUMMARY

CTP-0071, released 25 July 1988, outlined a two-phase test program designed to answer questions about the suspected fracture criticality of the RSRM nozzle actuator bracket. The need for this testing became apparent after performing a fracture mechanics analysis of the actuator bracket. The analysis showed that with a preexisting crack of 0.10 in., the bracket would fail on the first occurrence of actuator stall load. This size of crack is equal to the detectability limit of the dye penetrant method used for inspection of the bracket.

It was not known how well the analytical model represented real actuator bracket behavior. The decision was made to perform the necessary tests to answer this question. It was also decided to design the testing in such a way as to directly verify the ability of the actuator bracket to meet the requirements regarding fatigue crack growth.

Phase 1 of the testing addressed the accuracy of the analytical model. The test specimen was a pin-loaded square lug designed to represent the analytical model. Test results showed that the analytical model was conservative by a factor of 2.0 to 3.0 for predicting failure loads in the crack size range of interest. For crack sizes ranging from 0.075- to 0.2-in. surface length, the experimental failure loads ranged from 157,400 to 119,000 lb, respectively (Figure 1). The analytical predictions ranged from 64,000 to 41,000 lb, respectively.

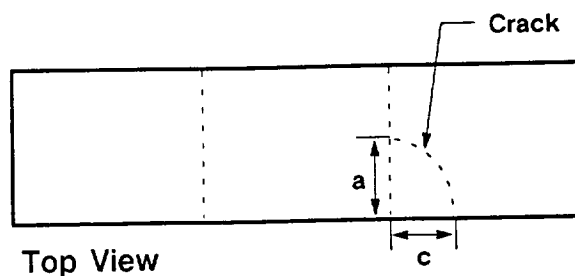
Certification of the actuator bracket's fracture mechanics safe-life requirements was conducted in Phase 2 of testing.

Four Phase 2 tests were planned, but only two were completed before a test fixture failure prompted the cancellation of the remaining tests. The two successful tests, using flight-configured actuator brackets (Drawing No. 1U51242), demonstrated compliance with the fracture mechanics safe-life requirements. Actuator bracket (Drawing No. 1U75643) was not tested, however, the difference in the configuration of the two brackets does not have a structural impact on the test results. Both brackets are qualified. The tests verified that the bracket could withstand four cyclings of the flight load spectrum while having a preexisting 0.11-in. crack at the suspected critical location. Tests included actuator stall loads.

3.2 CONCLUSIONS

3.2.1 Phase 1 Conclusions

<u>Test Objective</u>	<u>Conclusion</u>
Verify lug fracture predictions of NASA/FLAGRO linear elastic fracture mechanics analytical model.	<i>Verified.</i> Analytical model is conservative by a factor of 2.0 to 3.0 critical load for the crack size range of interest.
Determine critical load in square lug specimen for various initial crack sizes.	<i>Determined.</i> Results listed in Figure 1.
Determine the acceptability of the lug model for analyzing the actuator bracket.	<i>Determined.</i> The lug model is not acceptable for analysis when linear elastic assumptions are violated. Results are conservative by a factor of 2.0 to 3.0 critical load.



Specimen	c (in.)	a (in.)	Failure Load (lb)
1	0.075	0.095	157,387
2	0.075	0.090	158,089
3	0.090	0.115	153,088
4	0.195	0.270	119,089
5	0.100	0.155	146,975
6	0.215	0.315	126,006

A038272a

Figure 1. Phase 1 Testing Results

3.2.2 Phase 2 Conclusions

Test Objective

Verify capability of actuator bracket to undergo four cycles of the flight load spectrum with a 0.10 by 0.10-in. radius preexisting corner crack.

Determine the critical load for the actuator bracket with a 0.10 by 0.10-in. crack.

Determine the critical flaw size in the actuator bracket at the actuator stall load (103,424 lb).

Conclusion

Verified. Test specimen 2-1 (Figure 2) survived four cycles of a load spectrum equivalent to flight load spectrum (reference Attachment A) and afterwards did not fail under a static load of 237,000 lb. Pre-cracking loads applied to test specimen 2-2 (Figure 3) did not produce fatigue crack initiation at the starter notch. Testing was not continued for this specimen.

Test was cancelled per NASA memo SA51(192-90) due to test fixture failure (Attachment B).

Test was cancelled per NASA memo SA51(192-90) due to test fixture failure (Attachment B).

3.3 RECOMMENDATIONS

Test results of this test verify that the actuator bracket is qualified to undergo four cycles of the flight load spectrum with a 0.10 by 0.10-in. radius preexisting corner crack.

It is recommended that the assumptions of linear elastic fracture mechanics be checked for validity when using the NASA/FLAGRO model. It is also recommended that the results obtained using the NASA/FLAGRO model be validated by testing and additional analysis techniques.

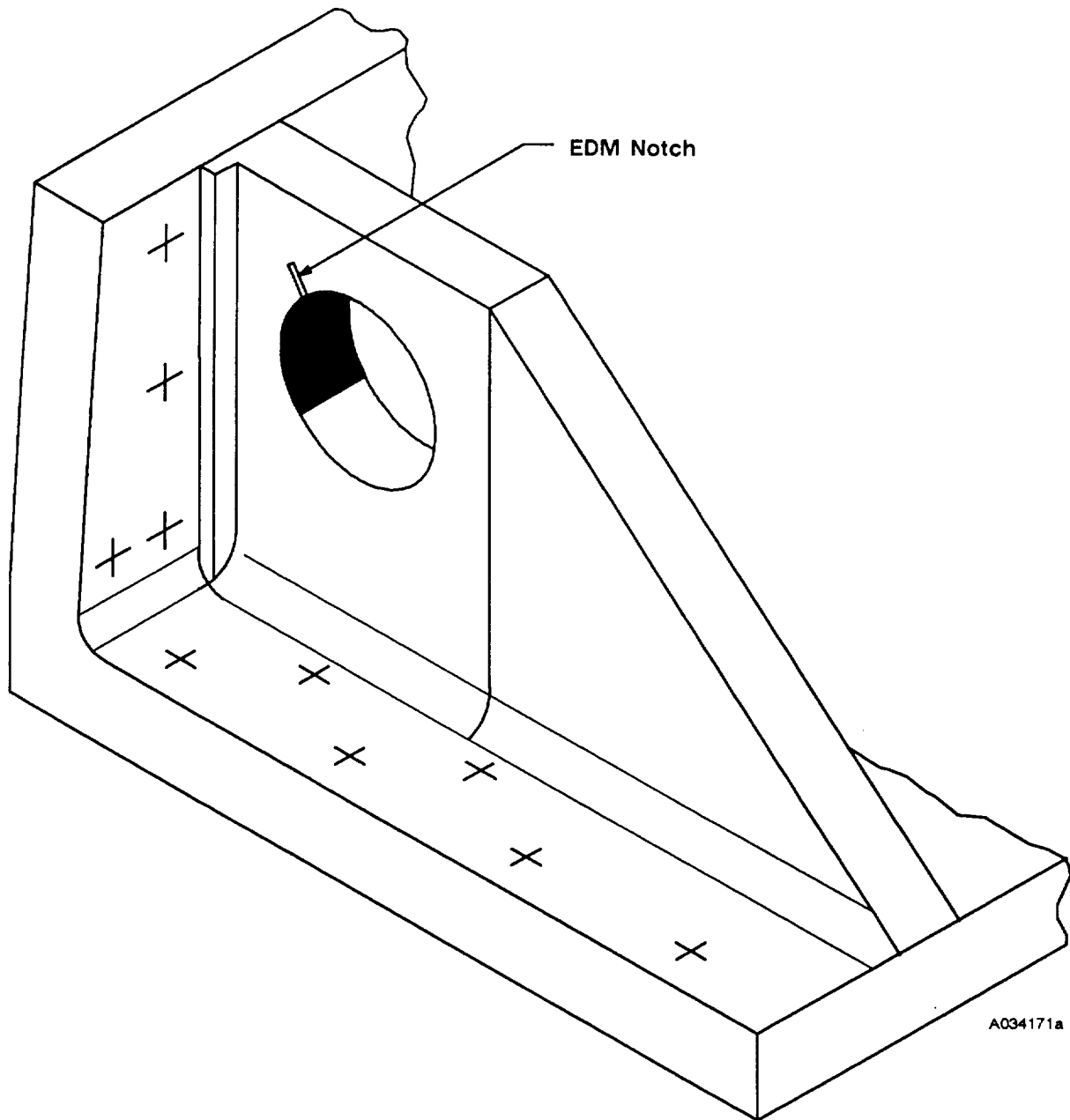


Figure 2. Specimen 2-1 Starter Notch Location

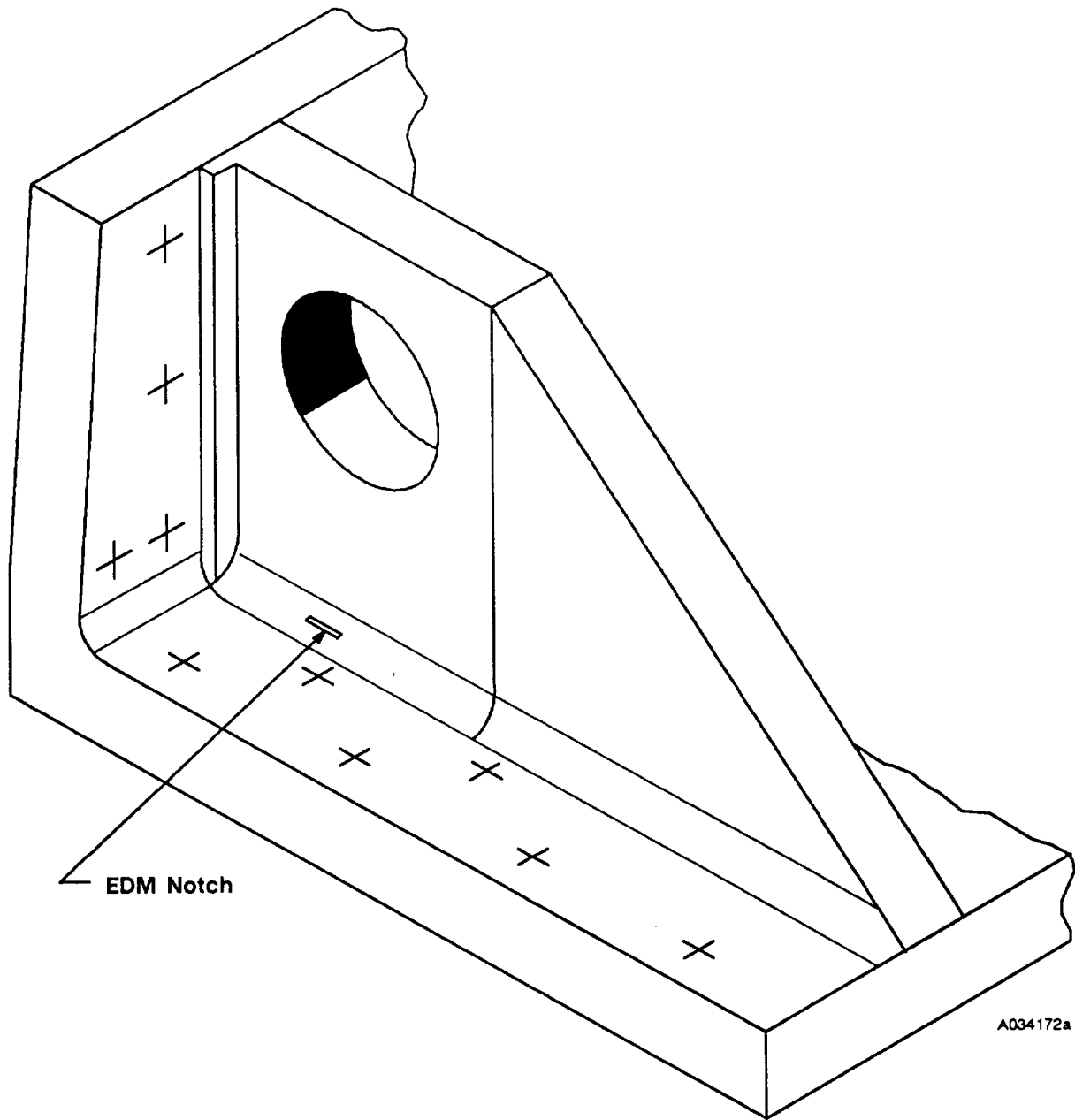


Figure 3. Specimen 2-2 Starter Notch Location

4 / INSTRUMENTATION

Instrumentation measurements for Phases 1 and 2 consisted of:

- A. Applied load
- B. Displacement
- C. Crack length
- D. Number of loading cycles
- E. Strain

Load cells were used for both cyclic and static loading measurements. Displacement measurements were made using the testing machine's ability to measure crosshead displacement. Strain measurements were taken with strain gages bonded to test specimens 2-1 and 2-4. Crack surface length was measured with an optical microscope.

5 / PHOTOGRAPHY

Still black and white photographs of the test specimens were taken. Copies of the photographs (Series No. 117798) are available from the Thiokol Corporation Photographic Services department.

6 / TEST ITEM DESCRIPTION

Testing was conducted in two phases. In Phase 1 six square lug specimens, constructed of 1.0-in. thick 7075-T73 rolled aluminum plate, were tested. Phase 2 test specimens were flight-configured actuator brackets (Drawing No. 1U51242). The bracket was machined from a single rough forging of 7075-T7351 aluminum.

To facilitate fatigue crack initiation in the desired location, starter notches were cut in the specimens using an electrical discharge machining (EDM) process. Fatigue cracks were induced by cyclically loading the test specimens. The loads used to initiate and grow the fatigue cracks prior to testing (precracking loads) were determined in accordance with ASTM-E399-83. After precracking, each specimen was statically loaded to failure. The peak load and a load versus crosshead displacement curve was recorded during the failure loading.

The difference between the minimum flight temperature of 65°F for the actuator bracket area and the ambient test environment is insignificant.

6.1 PHASE 1 TESTING

Phase 1 investigated the accuracy of the NASA/FLAGRO pin-loaded lug fracture mechanics model. The test specimens were designed to duplicate the analytical model. Figure 4 illustrates the configuration of the NASA/FLAGRO model.

The model consisted of a square lug, pin-loaded through the central hole. A corner crack existed at the corner of the pin-loaded hole in the plane normal to the loading direction. The dimensions shown in Figure 4 were chosen to represent actuator bracket behavior using a simple square lug model. Figure 5 illustrates how the square lug model relates to the real actuator bracket.

The Phase 1 test specimen and apparatus is shown in Figures 6 and 7. The lower portion of the aluminum specimen was clamped tightly between two steel plates, providing a rigidly fixed boundary condition at the lower edge of the specimen's upper lug region.

6.2 PHASE 2 TESTING

Three of the four Phase 2 specimens were notched in a location adjacent to the actuator attachment hole (Figure 2). Specimen 2-3 was given two notches, one on each side of the bracket while specimens 2-1 and 2-4 were given a single notch on only one bracket flange. The EDM notch in specimen 2-2 was located in the fillet at the base of one of the bracket flanges where it joins the bracket base (Figure 3).

The test apparatus (Figure 8) was designed to simulate the loading experienced by the actuator bracket during nozzle vectoring.

Two of the specimens were tested before a failure in the test fixture prompted the cancellation of the remaining tests. The specimens tested were those designated as 2-1 and 2-2 in CTP-0071. Since these specimens were directly related to the qualification objective, it was decided that continued testing was not necessary.

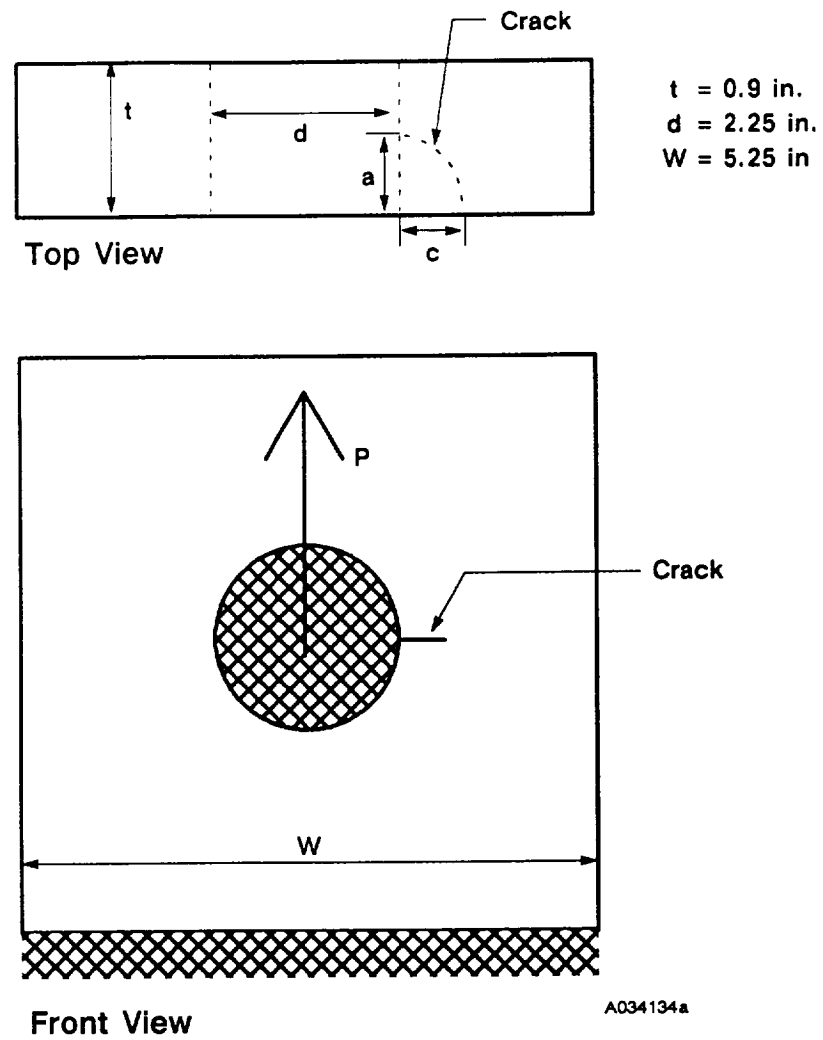


Figure 4. Square Lug Mode/Test Specimen Geometry Dimensions

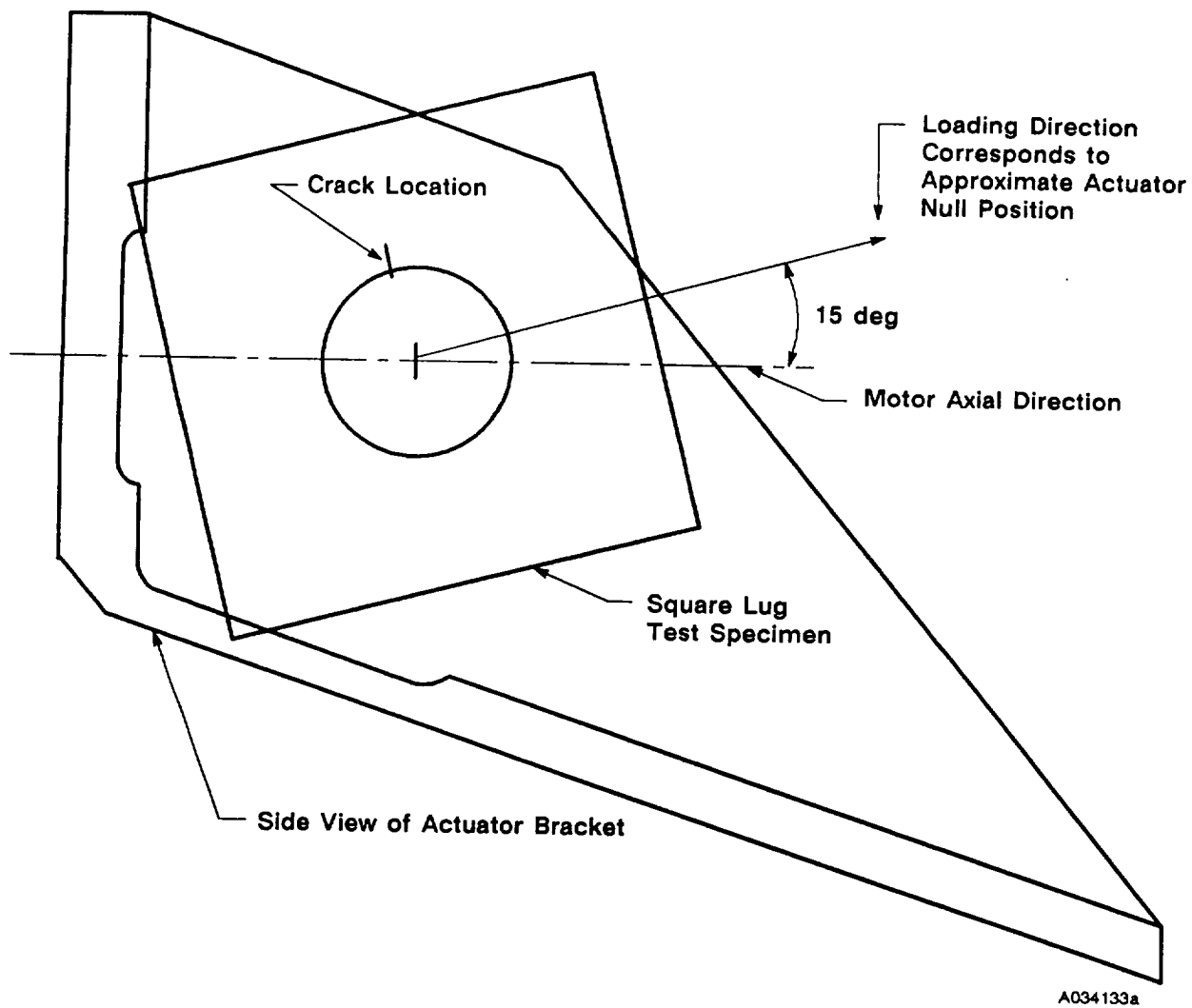
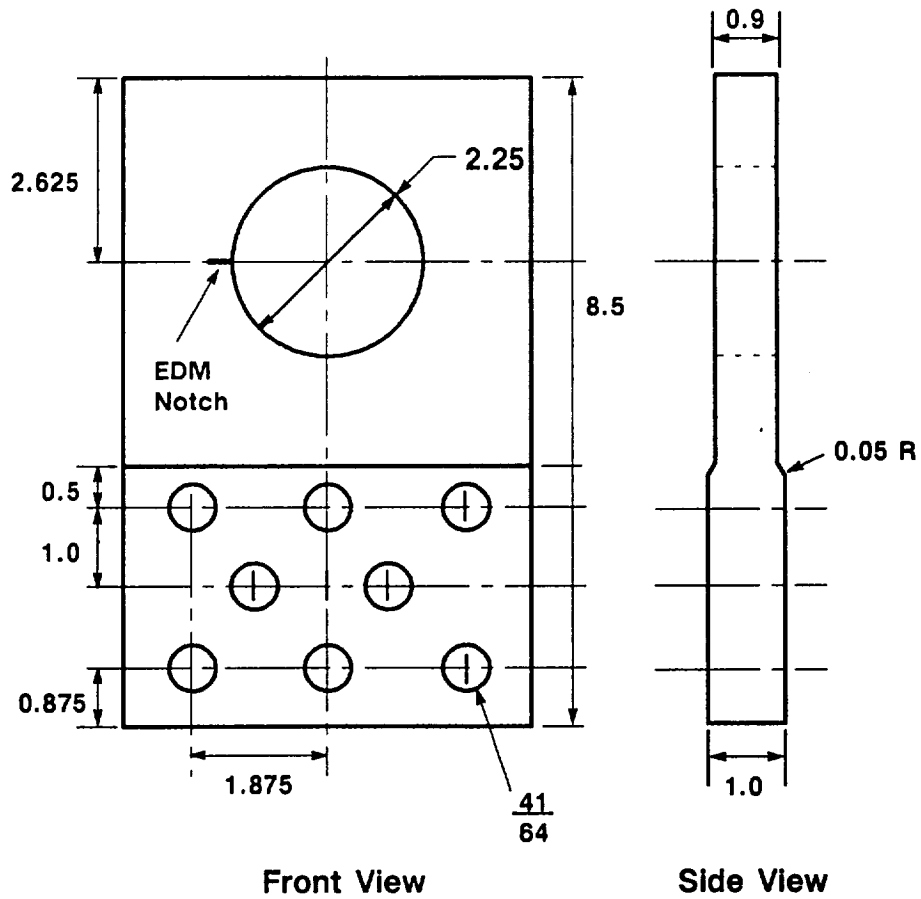


Figure 5. Comparison of Analytical Model to Actuator Bracket



A034168a

Figure 6. Phase 1 Test Specimen

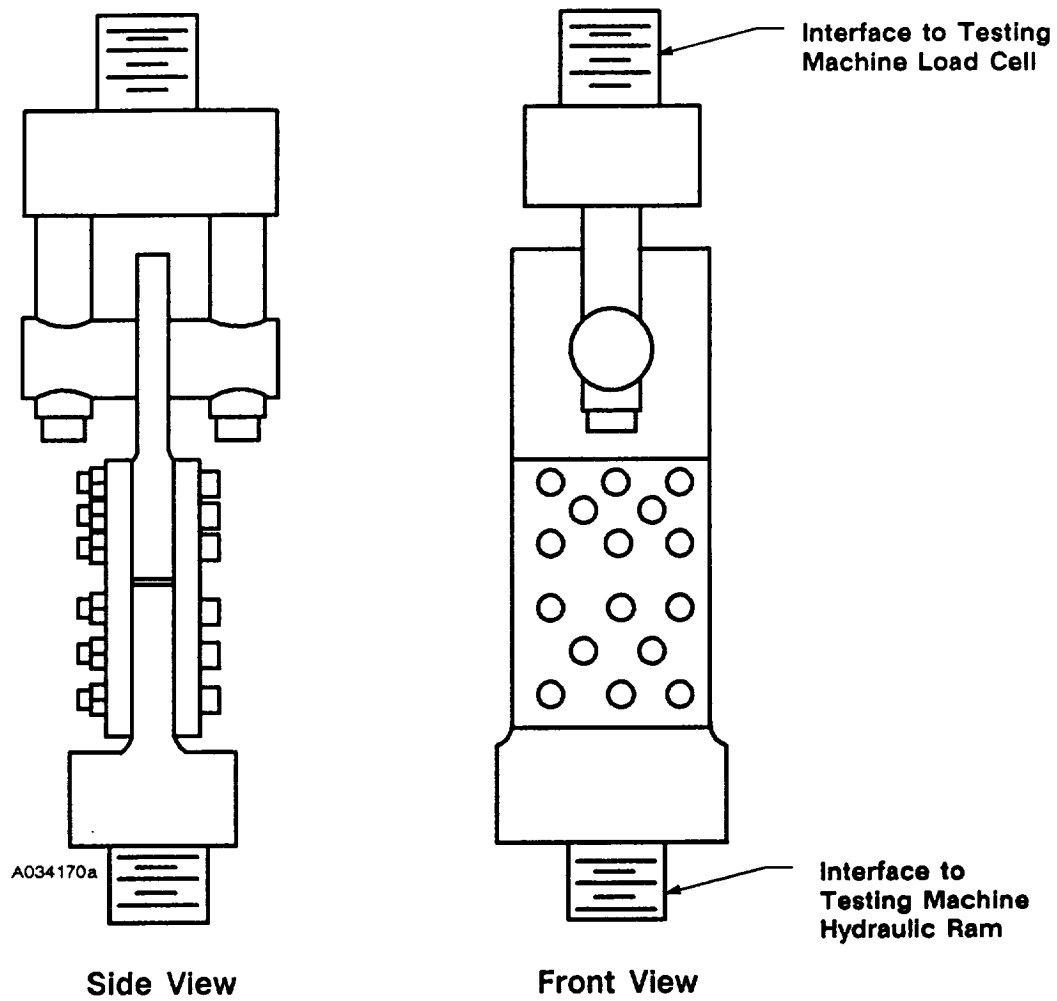


Figure 7. Phase 1 Test Fixture

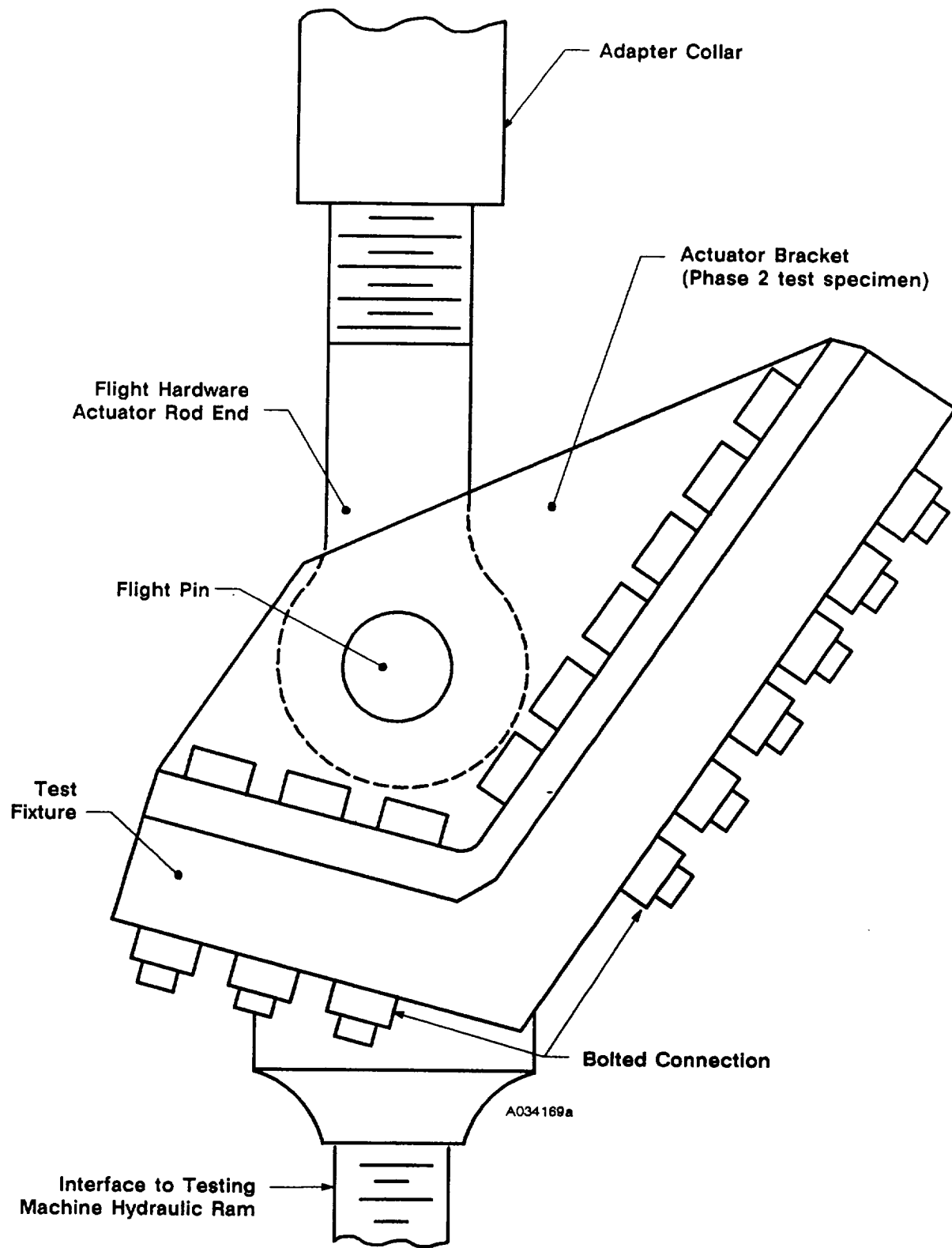


Figure 8. Phase 2 Test Specimen and Configuration

RESULTS AND DISCUSSIONS

7.1 PHASE 1

The specific objectives of Phase 1 were to determine the accuracy of the lug fracture predictions from the NASA/FLAGRO fracture mechanics model and to determine critical loads in the square lug test specimen for three different initial crack sizes.

7.1.1 Analytical Model

To investigate the accuracy of the analytical model for Phase 1 applications, the actual crack sizes from each test specimen were analyzed with the NASA/FLAGRO model. The corner cracked lug model produces a solution for the stress intensity at each of the two ends of the crack front where it intersects the surface of the lug. The solution was assumed to represent the critical condition when either one of the two stress intensity values became equal to the fracture toughness of the material. A value of 26 ksi $\sqrt{\text{in.}}$ was used for the fracture toughness of 7075-T73 aluminum. This value was taken from the material property database contained in the NASA/FLAGRO program. This value is for the T-L orientation of the material which corresponds to the orientation of the cracks relative to the grain orientation in the specimens.

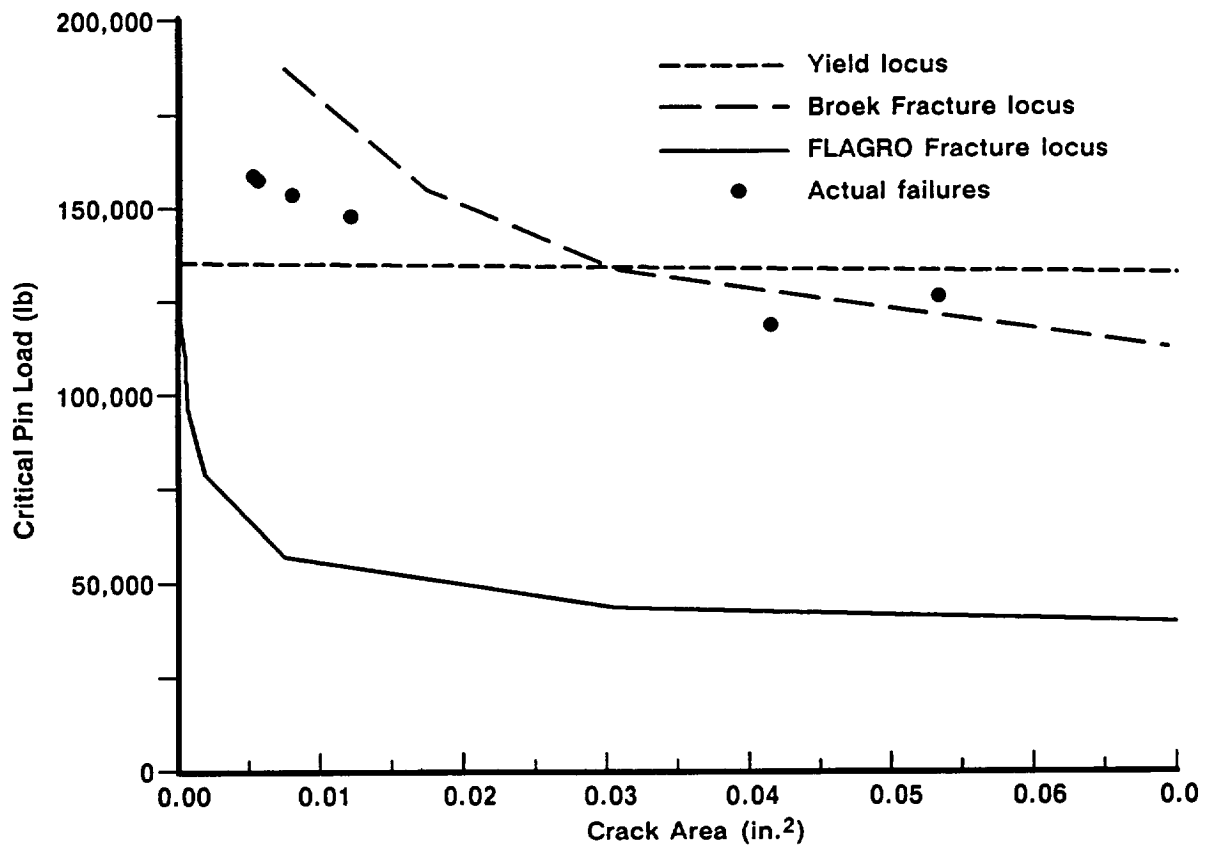
Figure 9 is a plot of the failure load versus crack area, showing actual specimen failure points, the net section yield locus, and two different fracture loci. The yield locus is based on a yield stress of 50 ksi and perfectly plastic postyield behavior. One of the fracture loci is computed using the NASA/FLAGRO solution while the other is computed from an engineering solution (Reference B). This engineering solution is applicable to small corner cracks emanating from holes. The NASA/FLAGRO solution is based on an empirical fit to experimental data from Johnson Space Flight Center.

Neither the simple net section yield approximation nor the NASA/FLAGRO model is adequate to describe the failure process occurring in the Phase 1 specimens. The engineering solution (Reference B) provides the closest agreement to the experimental data. However, the engineering solution is significantly in error in the region where yield-dominated failures would be expected.

7.1.2 Critical Loads

Pre-cracks for six Phase 1 specimens were grown to three different target sizes, 0.075, 0.10, and 0.20 inch. These measurements were made along the exposed surface of the test specimen. The specimens were then statically loaded until failure. The failure loads and the actual dimensions of the fatigue pre-cracks were recorded. Results of these tests are in Figure 1. Figures 10 through 15 are photomicrographs of the fracture surfaces of each failed specimen. The EDM starter notches and fatigue pre-cracks are visible in the photographs.

Residual Strength Square Lug With Corner Crack



A038271a

Figure 9. Comparison of Failure Load Versus Crack Area

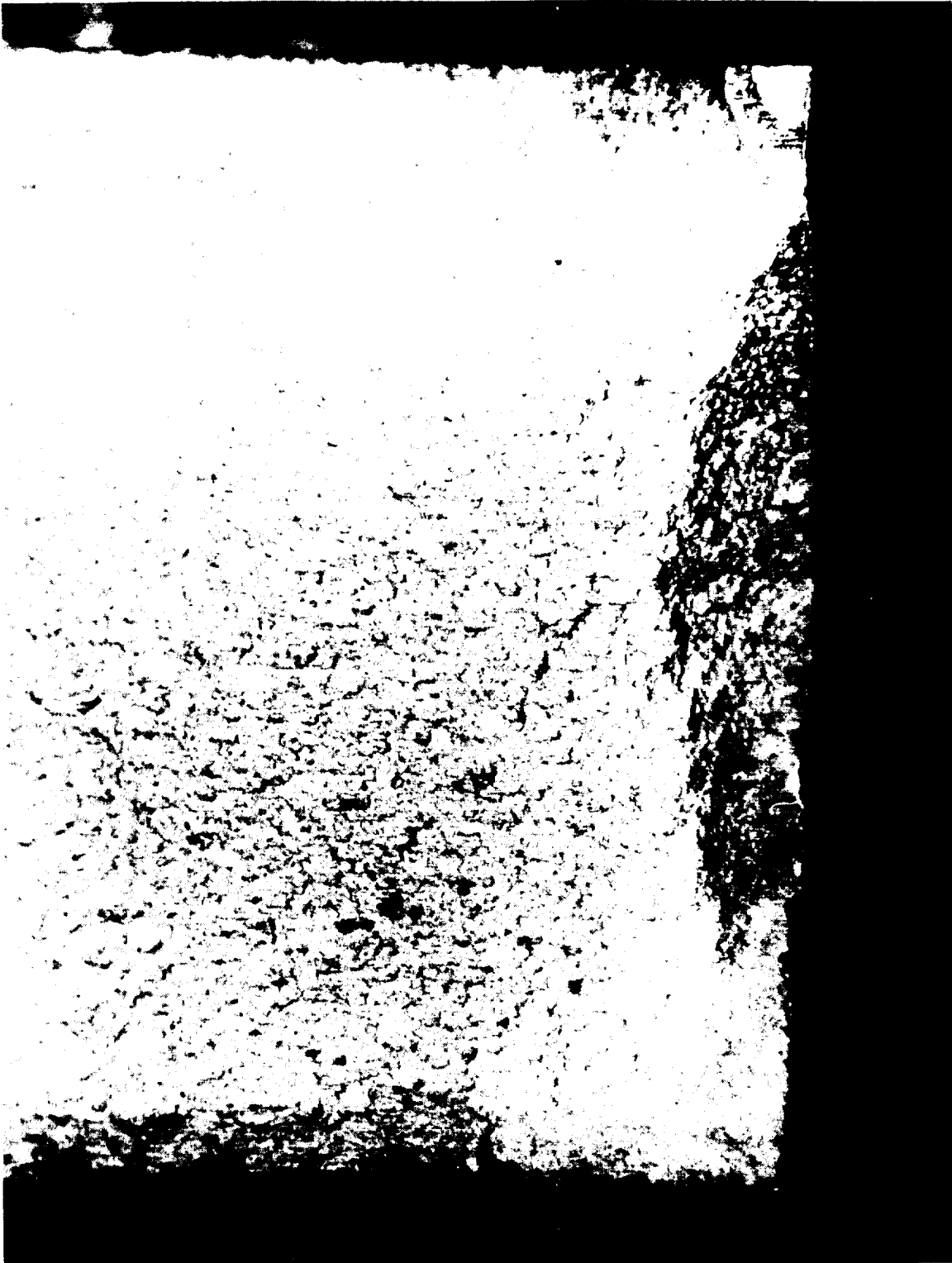


Figure 10. Phase 1 Post-test, Specimen 1



Figure 11. Phase 1 Post-test, Specimen 2



Figure 12. Phase 1 Post-test, Specimen 3



Figure 13. Phase 1 Post-test, Specimen 4



Figure 14. Phase 1 Post-test, Specimen 5



Figure 15. Phase 1 Post-test, Specimen 6

The results show that the corner cracked lug fracture mechanics solution contained in the NASA/FLAGRO model is conservative by a factor of 2.0 to 3.0 for predicting critical loads in 7075-T73 aluminum. The reason for these conservative results is the violation of linear elastic assumptions which are needed to ensure the validity of the analytical model.

The method of linear elastic fracture mechanics is valid only when the crack tip plastic zone is small, relative to the crack size. For 7075-T73 aluminum, this assumption is not valid for the crack sizes used in this test.

7.2 PHASE 2

The specific development objectives called for determining the critical load of a flight-configured actuator bracket (Drawing No. 1U51242) with an initial corner crack of 0.10 in., and determining the critical flaw size in a flight-configured actuator bracket (Drawing No. 1U51242) at the actuator stall load. However, these development objectives were not satisfied due to a test fixture failure before the testing was conducted.

The qualification objective for Phase 2 was to verify the capability of the actuator bracket to withstand four applications of the flight load spectrum with an initial corner crack of 0.10 inch.

Specimen 2-1 contained an EDM starter notch adjacent to the actuator attachment hole (Figure 2). Approximately 12,000 cycles of pre-cracking load were required to grow a fatigue pre-crack of 0.10 in. length on exposed surface of bracket.

Four cycles of the flight load spectrum (Table 1) were applied to specimen 2-1 following measurement of the pre-crack. Four cycles of the flight load spectrum (Table 1) were applied to specimen 2-1 following measurement of the precrack. This load spectrum is not identical to the load spectrum identified in TWR-16801. The reasons for this difference are the following:

- a. The load simulated in CTP-0071 is from TWR-16975 (Tables 8.1-1 through 8.1-5), not from TWR-16801, Rev. B, Vol. II. At the time the test plan was written, TWR-16975 was the only available source of the fatigue flight load spectrum.
- b. There are discrepancies between CTP-0071 load spectrum and TWR-16975 flight load spectrum:
 - There were typographical errors in the number of cycles.
 - Some loads were left out because of no cyclic loads.
 - Accelerations were not included. (See details in Attachment A, Table 1, Page A-8)

Fracture mechanics crack growth analyses (see Attachment A) were performed to compare CTP-0071 load spectrum with load spectrum specified in TWR-16801. CTP-0071 simulates flight loads. The NASA/FLAGRO program was used in the analyses.

Table 1. Flight Load Spectrum

Load Step	Mean Load (lb)	Amplitude (lb)	Minimum Load (lb)	Maximum Load (lb)	Cycles
1	29,100	16,800	12,300	45,900	5
2	29,100	5,600	23,500	34,700	5
3	29,100	1,600	27,500	30,700	2
4	29,100	2,600	26,500	31,700	14
5	29,100	3,600	25,500	32,700	4
6	29,100	600	28,500	29,700	89
7	29,100	1,200	27,900	30,300	101
8	29,100	1,800	27,300	30,900	30
9	29,100	800	28,300	29,900	84
10	29,100	1,500	27,600	30,600	101
11	29,100	2,300	26,800	31,400	30
12	39,900	16,500	23,400	56,400	13
13	39,900	5,200	34,700	45,100	52
14	39,900	1,200	38,700	41,100	94
15	39,900	2,200	37,700	42,100	28
16	39,900	3,200	36,700	43,100	323
17	39,900	600	39,300	40,500	394
18	39,900	1,200	38,700	41,100	103
19	39,900	1,900	38,000	41,800	103
20	39,900	800	39,100	40,700	323
21	39,900	1,500	38,400	41,400	394
22	39,900	2,300	37,600	42,200	103
23	0	1,100	-1,100	1,100	101
24	0	1,700	-1,700	1,700	122
25	0	2,300	-2,300	2,300	37
26	0	2,500	-2,500	2,500	90
27	0	4,300	-4,300	4,300	108
28	0	6,000	-6,000	6,000	32
29	0	700	-700	700	203
30	50,000	50,000	0	100,000	1

The results presented in Attachment A, Table 2, Page A-11 indicated that after four mission cycles of loading, the stress intensity factors caused by the required load spectrum are higher than the CTP-071 load spectrum by three percent. This is because the required actuator stall load is 103,424 lb whereas the CTP-071 stall load is only 100,000 lb (due to machine capability limitation). However, it is still smaller than the fracture toughness of the material, according to the results from Phase 1 of CTP-0071. The required load spectrum would make an initial corner crack of 0.10 in. grow to 0.100173 in., whereas CTP-0071 load spectrum would make the same initial corner crack grow to 0.100168 in. which is only 0.005 percent less than 0.100173 inch.

The effect of the CTP-0071 load spectrum is equivalent to the required load spectrum. Consequently, the results from CTP-0071 can be used to qualify the actuator bracket.

The flight loading resulted in approximately 0.004 in. of additional crack growth. The bracket was then statically loaded to 237,000 lb in an attempt to fail the bracket at the crack. Failure of the test fixture at 237,000 lb forced the test to be terminated prior to test specimen failure. There was approximately 0.006 in. of crack extension following application of the static load.

The damage to the test fixture was so severe that major repairs would have been required for testing to resume. Since the qualification objective had been successfully accomplished, further testing was canceled per NASA memo SA51(192-90) (Attachment A).

Specimen 2-2 contained an EDM starter notch located in the fillet at the base of the bracket web where it meets the bracket base plate (Figure 3). A pre-cracking load was applied to specimen 2-2 for 500,000 cycles in an attempt to initiate fatigue crack growth at the starter notch. No fatigue crack initiation was produced during this period, resulting in the conclusion of testing specimen 2-2.

8

APPLICABLE DOCUMENTS

CTP-0071	RSRM Nozzle Actuator Bracket/Lug Fracture Mechanics Qualification Test Plan
TWR-15723	Development and Verification Plan for the Redesigned Solid Rocket Motor
CPW1-3600A	Prime Equipment Contract End Item (CEI) Detail Specification
TWR-16875	Fracture Control Plan for Space Shuttle RSRM Nozzle
ASTM E399-83	Standard Test Method for Plane-Strain Fracture Toughness of Metallic Materials
Reference 1	Broek, D., Elementary Engineering Fracture Mechanics, Third Edition, The Hague, 1983, pp. 352-356
SA51(192-90)	NASA Memo Canceling Further Testing (Attachment B)

Attachment A

Thiokol CORPORATION
SPACE OPERATIONS

24 May 1993
L633-FY93-M112 Rev. A

TO: K. F. Lueders
Systems Planning and Interfaces

CC: G. M. Berhold, D. E. Campbell, R. V. Cook, J. V. Daines,
T. K. Lai, B. Paul, K. W. Stephens, R. K. Wilks

FROM: T. T. Nhan
Nozzle Structural Analysis

SUBJECT: Crack Growth Comparison between Actuator Bracket CTP-0071 Load
Spectrum and Required Fatigue Flight Load Spectrum

REFERENCES:

- A. Kelly, S., CTP-0071 Revision C, "RSRM Nozzle Actuator Bracket/Lug Fracture Mechanics Qualification Test Plan," 25 July 1988.
- B. McCormack, J. D., Interoffice Memo L711-FY93-M348, "Nozzle Actuator Fatigue Loads," 23 February 1993. (Attached)
- C. McCormack, J. D., TWR-16801 Volume 2 Revision A, "RSRM Design Loads Data Book - Volume 2: Post-Separation, Fatigue, and Interface Loads," Thiokol Corporation, To be released.
- D. Composite Group, TWR-16975 Rev. B, "RSRM Nozzle Stress Report," Morton Thiokol, Inc., 1 February 1989.
- E. Rebello, C. J. and Phipps B. E., TWR-15995, "Space Shuttle RSRM Nozzle Materials Data Book," Morton Thiokol, Inc. 19 January 1989.
- F. Jensen, K. R., and Richards, M. C., TWR-10211, "Mass Properties Quarterly Status - Space Shuttle Solid Rocket Motor," Thiokol Corporation, 5 March 1993.

1.0 INTRODUCTION

Concern has been raised whether CTP-0071 (see Reference A) test results can be used to qualify the actuator bracket as it was intended. The reason for the concern is that the flight load spectrum simulated by CTP-0071 is not the

same as the required flight load one as documented in Interoffice Memo L711-FY93-M348, dated 23 February 1993 (see Reference B) which will be incorporated in TWR-16081 Vol. 2 Rev.B (see Reference C).

This memo is to document the crack growth analyses of the fatigue load spectrum simulated by CTP-0071 and the required load spectrum and corresponding conclusion.

The memo is revised because there were two errors in the number of cycles of the required flight load spectrum.

2.0 BACKGROUND INFORMATION

As stated in CTP-0071, one of the test objectives is: "to verify the capability of actuator bracket to undergo four cycles of the flight load spectrum with a 0.10 inch pre-existing crack." However, the flight load spectrum in CTP-0071 is different from the actual required flight load spectrum.

The reasons for this discrepancy are the following:

- (a) The load simulated in CTP-0071 is from TWR-16975 (see Reference D, Tables 8.1-1 through 8.1-5), not from TWR-16801 (see Reference C). At the time the test plan was written, TWR-16975 was the only available source of the fatigue flight load spectrum because the required fatigue load spectrum, which will be presented in TWR-16801 Volume 2 Revision B (see Reference C), did not exist.
- (b) There are discrepancies between CTP-0071 load spectrum and TWR-16975 flight load spectrum:
 - Several errors are typos in the number of cycles;
 - Some loads were left out because of no cyclic loads.
 - Accelerations were not included.See more details in Table 1.

3.0 SUMMARY AND CONCLUSION

Fracture mechanics crack growth analyses were performed to compare CTP-0071 load spectrum, intended to simulate flight loads, and the required load spectrum specified in Interoffice memo L711-FY93-M348 (see Reference B). The NASA/FLAGRO program was used in the analyses. The crack growth model is presented in Figure 1. The results are presented in Table 2.

The results indicated that after four mission cycles of loadings, the stress intensity factors caused by the required load spectrum are higher than the one caused by CTP-0071 load spectrum by three percent. This is because the required actuator stall load is 103,424 lbs whereas the CTP-0071 simulated

actuator stall load is only 100,000 lbs. However, it is still smaller than the fracture toughness of the material, according to the results from phase 1 of CTP-0071. The required load spectrum would make an initial corner crack of 0.10 inch grow to 0.100173 inch, whereas CTP-0071 load spectrum would make the same initial corner crack grow to 0.100168 inch which is only 0.005% less than 0.100173 inch.

Therefore, the effect of the CTP-0071 load spectrum is equivalent to the required load spectrum. Consequently, the results from CTP-0071 can be used to qualify the actuator bracket.

4.0 ANALYSIS RESULTS

The crack growth analysis results are presented in Table 2. A four block was selected. One block is equivalent to a one flight mission load spectrum.

Table 2 shows that the stress intensity factors caused by the required load spectrum are higher than the one caused by the CTP-0071 load spectrum by three percent. But it is still smaller than the fracture toughness of the material according to the results from phase 1 of CTP-0071. This is contributed by the fact that the required actuator stall load is 103,424 lbs whereas the CTP-0071 simulated actuator stall load is only 100,000 lbs. However, after four cycles, the required load spectrum would make an initial corner crack of 0.10 inch grow to 0.100173 inch, whereas the CTP-0071 load spectrum would make the same initial corner crack grow to 0.100168 inch which is only 0.005% less than 0.100173 inch. Therefore, the effect of the CTP-0071 load spectrum is equivalent to the required load spectrum.

5.0 ANALYSIS DISCUSSION

5.1 Assumption:

The model for crack growth analyses is presented in Figure 1.

5.2 Analysis Procedure:

Crack growth analyses were performed using NASA/FLAGRO program to compare (a) Fatigue load spectrum from CTP-0071; and (b) The required load spectrum from Interoffice Memo L711-FY93-M348, "Nozzle Actuator Fatigue Loads," which will be incorporated in TWR-16801 Volume 2 Revision B.

5.2.1 CTP-0071 Load Spectrum

The crack model for the actuator bracket is from TWR-16975 and presented in Figure 1. The fatigue load spectrum is presented in Table 3.

The load in pound is converted to bearing stress as follows. For example in load step #1 from Table 3.

$$\sigma_{\text{min bearing}} = \frac{\text{Minimum Load} / 2}{D * t} \quad \dots(1)$$

where D = hole diameter = 2.25 inch
t = flange thickness = 0.91 inch
Minimum Load = 12,300 lbs
2 for two flanges

Substituting these numerical values in equation (1), we get:

$$\sigma_{\text{min bearing}} = 3.004 \text{ ksi}$$

as shown in the first line of Table 3.

5.2.2 The Required Fatigue Load Spectrum

The required fatigue load spectrum is presented in Table 4:

- L1: radial, tangential, and axial loads acting simultaneously;
- L2, L3, L4, L5, L6, L7, L8, L9, and L10 acting independently but not simultaneously;
- B1: radial, tangential, and axial loads acting simultaneously;
- B2, B3, B4, B5, B6, B7, B8, B9, and B10 acting independently but not simultaneously.

(For L1, L2, etc. notations see column 2 of Table 4).

From this load spectrum, there are 81 different possible load spectrums because load L2 through L10, and B2 through B10 acts independently. However, it was reduced to only one which is the worst load spectrum to be analyzed as presented in Table 5. The technical reasons for the reduction are as follows:

- (a) The most critical load direction is the axial direction because that is the direction of the actuator stall. Consequently, the crack whose direction is perpendicular to the axial direction is the most critical. For that crack, accelerations in tangential

24 May 1993

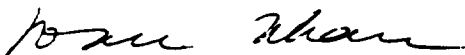
or radial directions have little or no effect on the crack growth. Consequently, accelerations in tangential and radial directions can be eliminated from the crack growth analysis.

- (b) Among axial accelerations (L8, L9, L10) and (B8, B9, B10), L10 and B10 are the worst. This is based on crack growth presented in Tables 7 and 8. L10 and B10 cracks grow the most.
- (c) The acceleration load itself is not significant. For example, the highest acceleration load is 30g which is equal to 780 lbs ($1g = 26$ lbs according to TWR-10211, Reference F). This is equivalent to a bearing stress of 190 psi, even for a 0.8 inch corner crack, the stress intensity factor is 0.5 ksi $\sqrt{\text{in}}$ (see calculation in Table 6). This stress intensity factor is much lower than the threshold stress intensity factor of 3.0 ksi $\sqrt{\text{in}}$. Also, 780 lbs is only 0.7 percent of the actuator stall load of 103424 lbs. (However, acceleration in the axial direction has been taken into account because it is the most critical direction.)

By the above reasoning, the load spectrum presented in Table 5, which is the worst, was established. Otherwise, eighty one analyses must be performed to analyze all possible combinations, unnecessarily, and the results would be the same.

5.3 Material Models:

Constitutive material properties and fracture mechanics properties of 7075-T73 aluminum used in the analyses are from TWR-15995 (see Reference E) except for the fracture toughness of aluminum, which was assumed at 50 ksi $\sqrt{\text{in}}$ for the comparison of the crack growth analysis.

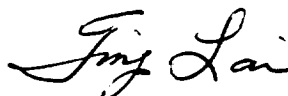


T. T. Nhan

Concurrence:



B. E. Phipps, Supervisor
Nozzle Structural Analysis



T. K. Lai, Chair
RSRM Fracture Control
Technical Subcommittee

/ev

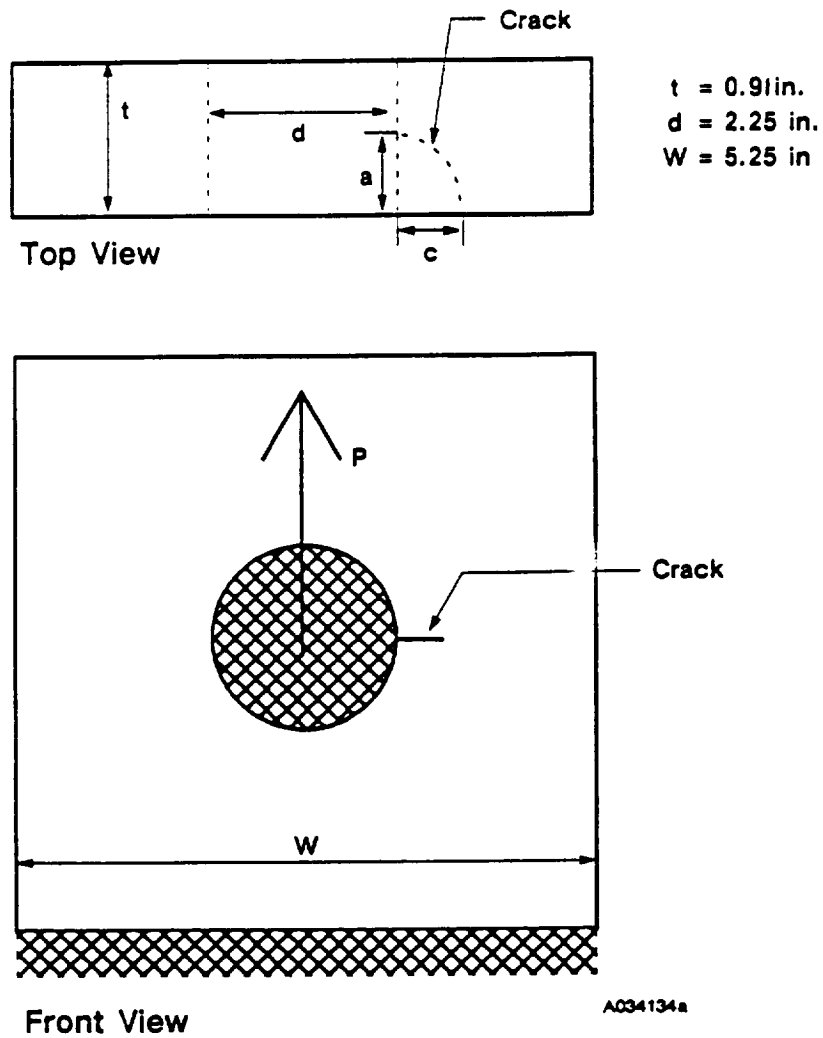


Figure 1 Crack Growth Analysis Model for the Actuator Bracket using NASA/FLAGRO Program

**Table 1 Comparison Between TWR-16975 Flight Load Spectrum
and CTP-0071 Simulated Load Spectrum**

TWR-16975 Load Spectrum										CTP-0071 Load Spectrum				
Mission Phase	Sequence	Actuator Load, lbs	Engine Gimbal, lbs	Low Freq + Random Vibration Loads		Total Applied Loads		# of Cycles	Sequence	Mean Load, lbs	Min Load, lbs	Max Load, lbs	# of Cycles	
					Tang		Tang							
Lift off	1	29,100	15,200	1,601	2,005	45,901	2,005	5	1	29,100	12,300	45,900	5	
	2	29,100	4,000	1,601	2,005	34,701	2,005	5	2	29,100	23,500	34,700	5	
	3	29,100	-----	1,601	2,005	30,701	2,005	2	3	29,100	27,500	30,700	2	
	4	29,100	-----	2,584	2,835	31,684	2,835	14	4	29,100	26,500	31,700	14	
	5	29,100	-----	3,572	3,679	32,672	3,679	4	5	29,100	25,500	32,700	4	
	6	29,100	-----	618	-----	29,718	-----	808	6	29,100	28,500	29,700	89	
	7	29,100	-----	1,236	-----	30,336	-----	1016	7	29,100	27,900	30,300	101	
	8	29,100	-----	1,855	-----	30,955	-----	306	8	29,100	27,300	30,900	30	
	9	29,100	-----	773	-----	29,873	-----	848	9	29,100	28,300	29,900	84	
	10	29,100	-----	1,546	-----	30,646	-----	1015	10	29,100	27,600	30,600	101	
	11	29,100	-----	2,318	-----	31,418	-----	306	11	29,100	26,800	31,400	30	
	12	29,100	-----	-----	829	29,100	829	848					..	
	13	29,100	-----	-----	1,659	29,100	1,659	1016					..	
	14	29,100	-----	-----	2,503	29,100	2,503	335					..	

Notes:

- * Errors in number of cycles.
- ** Not simulated.

Table 1 Comparison Between TWR-16975 Flight Load Spectrum
and CTP-0071 Simulated Load Spectrum (Continued)

TWR-16975 Load Spectrum									CTP-0071 Load Spectrum				
Mission Phase	Sequence	Actuator Load, lbs	Engine Gimbal, lbs	Low Freq + Random Vibration Loads		Total Applied Loads		# of Cycles	Sequence	Mean Load, lbs	Min Load, lbs	Max Load, lbs	# of Cycles
					Tang		Tang						
Re-entry	29	-----	-----	1,136	1,282	1,136	1,282	1010	23	0	-1100	1100	101
	30	-----	-----	1,679	1,282	1,679	1,282	1220	24	0	-1700	1700	122
	31	-----	-----	2,262	1,282	2,262	1,282	370	25	0	-2300	2300	37
	32	-----	-----	2,469	1,282	2,469	1,282	909	26	0	-2500	2500	90
	33	-----	-----	4,254	1,282	4,254	1,282	1080	27	0	-4300	4300	108
	34	-----	-----	6,043	1,282	6,043	1,282	320	28	0	-6000	6000	32
	35	-----	-----	726	2,367	726	2,367	820	29	0	-700	700	203
	36	-----	-----	726	3,453	726	3,453	920					..
	37			726	4,554	726	4,554	920					..
Actuator / Stall		103,424	-----	-----	-----	103,424	-----		30	50,000	0	100,000	1

Notes:

* Errors in number of cycles.

.. Not simulated.

.... Only 97 percent of the required actuator stall load.

**Table 1 Comparison Between TWR-16975 Flight Load Spectrum
and CTP-0071 Simulated Load Spectrum (Continued)**

CTP-0071 Load Spectrum													
Mission Phase	Sequence	Actuator Load, lbs	Engine Gimbal, lbs	TWR-16975 Load Spectrum				# of Cycles	Sequence	Mean Load, lbs	Min Load, lbs	Max Load, lbs	# of Cycles
				Low Freq + Random Vibration Loads		Total Applied Loads							
					Tang		Tang						
Boost	15	39,900	15,200	1,246	1,025	56,346	1,025	13	12	39,900	23,400	56,400	13
	16	39,900	4,000	1,246	1,025	45,146	1,025	13	13	39,900	34,700	45,100	52
	17	39,900	-----	1,246	1,025	41,146	1,025	52	14	39,900	38,700	41,100	94
	18	39,900	-----	2,232	1,855	42,132	1,855	94	15	39,900	37,700	42,100	28
	19	39,900	-----	3,220	2,669	43,120	2,669	28	16	39,900	36,700	43,100	323
	20	39,900	-----	618	-----	40,518	-----	3230	17	39,900	39,300	40,500	394
	21	39,900	-----	1,236	-----	41,136	-----	3040	18	39,900	38,700	41,100	103
	22	39,900	-----	1,855	-----	41,755	-----	1030	19	39,900	38,000	41,800	103
	23	39,900	-----	773	-----	40,673	-----	3230	20	39,900	39,100	40,700	323
	24	39,900	-----	1,546	-----	41,446	-----	3940	21	39,900	38,400	41,100	394
	25	39,900	-----	2,318	-----	42,218	-----	1030	22	39,900	37,600	42,200	103
	26	39,900	-----	-----	830	39,900	830	3230					..
	27	39,900	-----	-----	1,659	39,900	1,659	3940					..
	28	39,900	-----	-----	2,503	39,900	2,503	1030					..

Notes:

* Errors in number of cycles.

.. Not simulated.

... CTP-0071 incorrectly says 14,100 lbs, but according to Scott Kelly the testing was conducted at 41,400 lbs which is correct.

**Table 2 Crack Growth Comparison Between
Required Flight Load Spectrum and
CTP-0071 Simulated Load Spectrum**

Block #	Required Flight Load Spectrum		CTP-0071 Load Spectrum	
	a^* , in	k^{**} , ksi $\sqrt{\text{in}}$	a^* , in	k^{**} , ksi $\sqrt{\text{in}}$
1	0.100043	22.66	0.100042	21.91
2	0.100086	22.67	0.100084	21.91
3	0.100136	22.67	0.100126	21.91
4	0.100173	22.67	0.100168	21.92

Notes:

- * a = crack length
- ** k = stress intensity factor
- *** 1 block = 1 load spectrum

**Table 3 Bearing Stress Input for Crack Growth Analysis
for CTP-0071 Load Spectrum**

Load Step	Mean Load (lb)	Amplitude (lb)	Minimum Load (lb)	Maximum Load (lb)	Cycles	σ min, Ksi per each bearing	σ max, Ksi per each bearing
1	29,100	16,800	12,300	45,900	5	3.004	11.209
2	29,100	5,600	23,500	34,700	5	5.739	8.474
3	29,100	1,600	27,500	30,700	2	6.716	7.497
4	29,100	2,600	26,500	31,700	14	6.471	7.741
5	29,100	3,600	25,500	32,700	4	6.227	7.985
6	29,100	600	28,500	29,700	89	6.960	7.253
7	29,100	1,200	27,900	30,300	101	6.813	7.399
8	29,100	1,800	27,300	30,900	30	6.667	7.546
9	29,100	800	28,300	29,900	84	6.911	7.302
10	29,100	1,500	27,600	30,600	101	6.740	7.473
11	29,100	2,300	26,800	31,400	30	6.349	7.668
12	39,900	16,500	23,400	56,400	13	5.714	13.773
13	39,900	5,200	34,700	45,100	52	8.474	11.013
14	39,900	1,200	38,700	41,100	94	9.451	10.037
15	39,900	2,200	37,700	42,100	28	9.206	10.281
16	39,900	3,200	36,700	43,100	323	8.962	10.525
17	39,900	600	39,300	40,500	394	9.597	9.890
18	39,900	1,200	38,700	41,100	103	9.451	10.037
19	39,900	1,900	38,000	41,800	103	9.280	10.208
20	39,900	800	39,100	40,700	323	9.548	9.939
21	39,900	1,500	38,400	41,400	394	9.377	10.110
22	39,900	2,300	37,600	42,200	103	9.182	10.305
23	0	1,100	-1,100	1,100	101	-0.269	0.269
24	0	1,700	-1,700	1,700	122	-0.415	0.415
25	0	2,300	-2,300	2,300	37	-0.562	0.562
26	0	2,500	-2,500	2,500	90	-0.611	0.611
27	0	4,300	-4,300	4,300	108	-1.050	1.050
28	0	6,000	-6,000	6,000	32	-1.465	1.465
29	0	700	-700	700	203	0.171	0.171
30	50,000	50,000	0	100,000	1	0	24,420

Table 4 Required Fatigue Load Spectrum

Mission Phase	Case	Contributor or Subcase	Actuator Load		Actuator CG Direction	Acceleration		No. of Cycles/Mission of Oscillatory Load or Accel.
			Steady State (\pm kips) *	Oscillatory Load (\pm kips)		Oscillatory Accel. (\pm gs)		
Lift-off	L1	Low Frequency Vibration	29.1	N/A	Radial	7.3	30	
					Tang.	7.3	30	
					Axial	7.3	30	
	L2	Random Vibration	29.1	N/A	Radial	10.0	360	
	L3		29.1	N/A		20.0	1030	
	L4		29.1	N/A		30.0	310	
	L5		29.1	N/A	Tang.	5.5	360	
	L6		29.1	N/A		11.0	1030	
	L7		29.1	N/A		16.5	310	
	L8		29.1	N/A	Axial	8.0	360	
	L9		29.1	N/A		16.0	1030	
	L10		29.1	N/A		24.0	310	
	L11	Engine Gimbal	29.1	4.0	N/A	N/A	5	
L12		29.1	15.2	N/A	N/A	5		
L13		29.1	0.5	N/A	N/A	325		
Boost	B1	Low Frequency Vibration	39.9	N/A	Radial	1.3	200	
					Tang.	1.3	200	
					Axial	3.5	200	
	B2	Random Vibration	39.9	N/A	Radial	10.0	3430	
	B3		39.9	N/A		20.0	4140	
	B4		39.9	N/A		30.0	1230	
	B5		39.9	N/A	Tang.	5.5	3430	
	B6		39.9	N/A		11.0	4140	
	B7		39.9	N/A		16.5	1230	
	B8		39.9	N/A	Axial	8.0	3430	
	B9		39.9	N/A		16.0	4140	
	B10		39.9	N/A		24.0	1230	
	B11	Engine Gimbal	39.9	15.2	N/A	N/A	13	
B12		39.9	4.0	N/A	N/A	13		
B13		39.9	0.5	N/A	N/A	600		
Reentry	R1	Low Frequency Vibration	N/A	N/A	N/A	N/A	N/A	
	R2	Random Vibration	N/A	N/A	Radial	23.2	2.3×10^4	
	R3		N/A	N/A	Tang.	7.2	2.1×10^4	
	R4		N/A	N/A	Axial	8.0	2.5×10^4	
	R5	Engine Gimbal	N/A	N/A	N/A	N/A	N/A	
Single Event	S1	Actuator Stall	103.424	N/A	N/A	N/A	N/A	
	S2	Splashdown Maximum	530.0	N/A	N/A	N/A	N/A	
	S3	Splashdown Minimum	-360.0	N/A	N/A	N/A	N/A	

- Note:
1. Axial is parallel to the centerline of the booster (positive aft), see Figure 5.4.2-1.
 2. The steady state load can be either compressive or tension.
 3. Splashdown loads taken from worst case loads from previous sections.

**Table 5 Bearing Stress and Cycle Input from
Required Flight Load Spectrum**

Phase	Sequence	Mean, Ksi	Cyclic, Kips	Pmin, Kips	Pmax, Kips	σ min, Ksi on each bearing	σ max, Ksi on each bearing	# of Cycles	Case
Lift- Off	1	29.1	\pm 0.203	28.897	29.303	7.057	7.156	30	L1 w/o Radial & Tang. Accel
	2	29.1	\pm 0.624	28.476	29.729	6.954	7.259	310	L10
	3	29.1	\pm 4.0	25.1	33.1	6.129	8.083	5	L11
	4	29.1	\pm 15.2	13.9	44.3	3.394	10.818	5	L12
	5	29.1	\pm 0.5	28.6	29.6	6.984	7.228	225	L13
Boost	6	39.9	\pm 0.091	39.809	39.991	9.721	9.766	200	B1 w/o Radial & Tang. Accel
	7	39.9	\pm 0.624	39.276	40.524	9.701	9.896	1230	B10
	8	39.9	\pm 15.2	24.7	55.1	6.032	13.455	13	B11
	9	39.9	\pm 4.0	35.9	44.9	8.767	10.965	13	B12
	10	39.9	\pm 0.5	39.4	40.4	9.621	9.866	600	B13
	11	51.712	\pm 51.712	0	103.424	0	25.256	1	S1

Note: See Table 4, Column 2 for L1, L2 etc. notations.

**Table 6 Stress Intensity Calculation for 30g Axial
Acceleration Acting on the Actuator Bracket**

STRESS INTENSITY SOLUTION CHECK FOR CC03

(computed: NASA/FLAGRO, 1986 Aug version, 1989 Mar rev.)
U.S. customary units [inches, ksi, ksi sqrt(in)]

Plate Thickness, t = 0.9100
" Width, W = 5.2500
Hole Diameter, D = 2.2500

S0 : Average Bearing Stress
S0 = 0.1900

a	:	c	:	K (a)	:	K (c)
0.10000	:	0.10000	:	0.17043	:	0.15352
0.20000	:	0.20000	:	0.23115	:	0.18920
0.30000	:	0.40000	:	0.30916	:	0.22792
0.50000	:	0.50000	:	0.34225	:	0.24748
0.60000	:	0.60000	:	0.37617	:	0.27129
0.70000	:	0.70000	:	0.41380	:	0.30169
0.80000	:	0.80000	:	0.45891	:	0.34200

**Table 7 Crack Growth Comparison Between
Load Cases L8, L9 and L10**

Load* Case	Axial Acceleration Load	Axial*** Acceleration Input	Cycles	a** _{final} , in
L8	8g	800g	860	0.100031
L9	16g	1600g	1030	0.100812
L10	24g	2400g	310	0.101338

Note:

- * See Table 4, Column 2 for L8, L9, and L10 notations
- ** Initial Crack Length = 0.10 inch
- *** The loads were multiplied by 100 to see the effect of crack growth.

**Table 8 Crack Growth Comparison Between
Load Cases B8, B9 and B10**

Load Case	Axial Acceleration Load	Axial*** Acceleration Input	Cycles	a** _{final} , in
B8	8g	800g	3430	0.100125
B9	16g	1600g	4140	0.103317
B10	24g	2400g	1230	0.105460

Note:

- * See Table 4, Column 2 for B8, B9 and B10 notations
- ** Initial Crack Length = 0.1 inch
- *** The loads were multiplied by 100 to see the effect of crack growth.

Thiokol CORPORATION

SPACE OPERATIONS

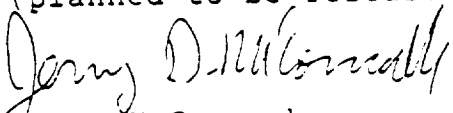
23 February 1993
L711-FY93-M348

TO: T. Nhan
Nozzle Structural Analysis


FROM: J. D. McCormack
System Analysis

SUBJECT: Nozzle Actuator Fatigue Loads

The table and figure in this memorandum (Table 5.4.2-1 and Figure 5.4.2-1), are the proposed table and figure to be placed in TWR-16801, Volume 2, Revision B. This data is provided to support release of a Design Engineering document that necessarily must be released prior to the release of TWR-16801, Volume 2, Revision B (planned to be released by the end of March).


J. D. McCormack
Systems Analysis

Concurrence:


D. R. Mason, Supervisor
Systems Analysis

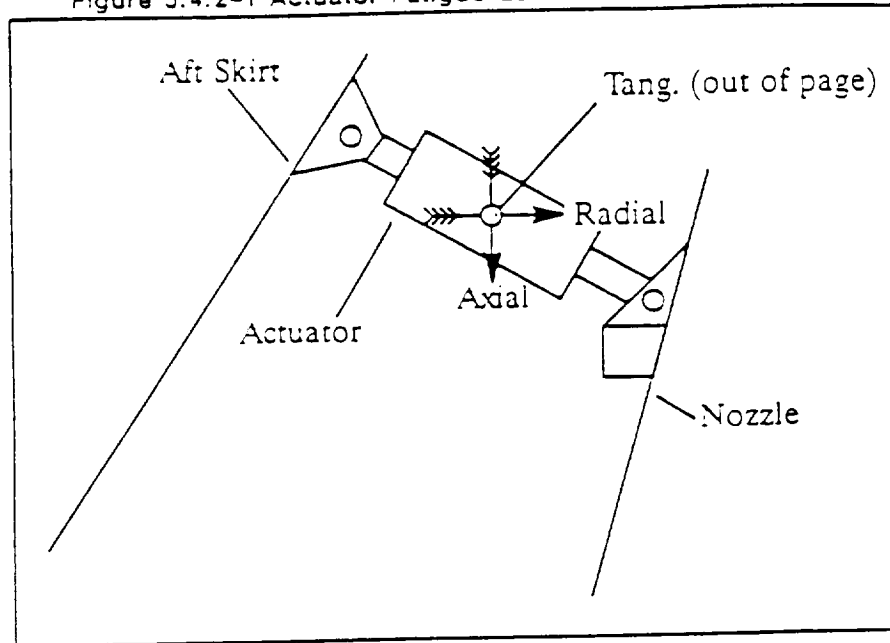
JDM/tlw

Table 5.4.2-1 Actuator Fatigue Loads Spectrum

Mission Phase	Case	Contributor or Subnase	Actuator Load		Actuator CG Direction ¹	Acceleration	No. of Cycles/Mission of Oscillatory Load or Accel.
			Steady State (\pm kips) ²	Oscillatory Load (\pm kips)		Oscillatory Accel. (\pm gs)	
Liftoff	L1	Low Frequency Vibration	29.1	N/A	Radial	7.3	30
					Tang.	7.3	30
					Axial	7.3	30
	L2	Random Vibration	29.1	N/A	Radial	10.0	350
	L3		29.1	N/A		20.0	1030
	L4		29.1	N/A		30.0	310
	L5		29.1	N/A	Tang.	5.5	350
	L6		29.1	N/A		11.0	1030
	L7		29.1	N/A		16.5	310
	L8		29.1	N/A	Axial	8.0	350
	L9		29.1	N/A		16.0	1030
	L10		29.1	N/A		24.0	310
	L11	Engine Gimbal	29.1	4.0	N/A	N/A	5
Boost	L12		29.1	15.2	N/A	N/A	5
	L13		29.1	0.5	N/A	N/A	225
	B1	Low Frequency Vibration	39.9	N/A	Radial	1.3	200
					Tang.	1.3	200
					Axial	3.5	200
	B2	Random Vibration	39.9	N/A	Radial	10.0	3430
	B3		39.9	N/A		20.0	4140
	B4		39.9	N/A		30.0	1230
	B5		39.9	N/A	Tang.	5.5	3430
	B6		39.9	N/A		11.0	4140
	B7		39.9	N/A		16.5	1230
	B8		39.9	N/A	Axial	8.0	3430
	B9		39.9	N/A		16.0	4140
Reentry	B10		39.9	N/A		24.0	1230
	B11	Engine Gimbal	39.9	15.2	N/A	N/A	13
	B12		39.9	4.0	N/A	N/A	13
	B13		39.9	0.5	N/A	N/A	600
	R1	Low Frequency Vibration	N/A	N/A	N/A	N/A	N/A
	R2	Random Vibration	N/A	N/A	Radial	23.2	2.3×10^3
	R3		N/A	N/A	Tang.	7.2	2.1×10^3
	R4		N/A	N/A	Axial	8.0	2.5×10^3
	R5	Engine Gimbal	N/A	N/A	N/A	N/A	N/A
	S1	Actuator Stall	103.424	N/A	N/A	N/A	N/A
	S2	Splashdown Maximum ³	530.0	N/A	N/A	N/A	N/A
	S3	Splashdown Minimum ³	-360.0	N/A	N/A	N/A	N/A

- Note:
1. Axial is parallel to the centerline of the booster (positive aft), see Figure 5.4.2-1.
 2. The steady state load can be either compressive or tension.
 3. Splashdown loads taken from worst case loads from previous sections.

Figure 5.4.2-1 Actuator Fatigue Loads Coordinate System



5.4.9 Igniter and Field Joint Heater Cables, Covers, and Channels

Fatigue loading for the igniter and field joint heater cables, covers, and channels are not applicable.

5.4.10 Propellant, Liner, Insulation, and Inhibitor

Fatigue loading for propellant, liner, insulation, and inhibitors are not applicable.

5.4.11 DFI/GEI

Fatigue loading for DFI/GEI are not contractually provided.

Attachment B

National Aeronautics and
Space Administration



George C. Marshall Space Flight Center
Marshall Space Flight Center, Alabama
35812

APR 19 1990

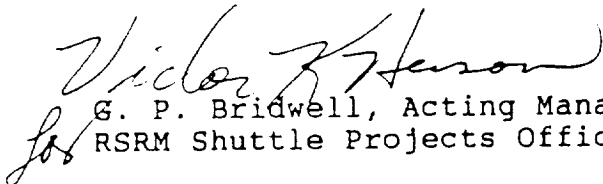
SA51(192-90)
Davis/4-5264

Thiokol Corporation
Attn: Mr. C. A. Speak
P. O. Box 707, M/S E60
Brigham City, UT 84302-0707

Subject: Actuator Bracket Fracture Mechanics Testing

Referenced is made to Thiokol letter E600-FY90-724, dated April 4, 1990, requesting authority to stop the nozzle actuator bracket fracture mechanics testing at this point in time. MSFC agrees that the qualification objectives of the test plan have been met by the phase-2 tests performed to date. It is not required that the testing related to development objectives be completed. Therefore, Thiokol Corporation is authorized to stop all testing associated with CTP-0071.

You are requested to prepare a final report summarizing the entire effort based on the work now completed.


G. P. Bridwell, Acting Manager
for RSRM Shuttle Projects Office

cc:
EA01/Mr. Schwinghamer
SA51/Mr. Henson/file
SA59/Mr. Skrobiszewski
EE51/Mr. Jones/file
EE52/Mr. Trenkle
EE53/Mr. Ross
EE54/Mr. Davis
EP54/Mr. Goldberg
AP46/Mr. Posey
TC-H/Mr. Brasfield

DISTRIBUTION

<u>Recipient</u>	<u>No. of Copies</u>	<u>Mail Stop</u>
G. Berhold	1	L82
D. Campbell	1	L71
F. Duersch	1	851
G. Laird	1	E68
P. Kelley	1	L71
T. Nhan	1	L63
T. Lai	1	L63
B. Phipps	1	L63
S. Kelly	1	L50
R. Papasian	31	E62A
G. Paul	1	L71
Data Management	1	L71F
Print Crib	5	MICRO